5. THE 2014/15 SNOWPACK DROUGHT IN WASHINGTON STATE AND ITS CLIMATE FORCING

Boniface O. Fosu, S.-Y. Simon Wang, and Jin-Ho Yoon

The 2014/15 snowpack drought resulted from exceedingly high temperatures notwithstanding normal precipitation—a drought type that may reoccur due to accelerated anthropogenic warming and aggravated by naturally driven low precipitation.

Introduction. The state of Washington declared a drought emergency in May 2015 following a drastic decline in snowpack over the adjoining Cascades (Fig. 5.1a). Unlike past droughts that were mainly caused by precipitation deficits (e.g., the 2005 drought; Anderson et al. 2006), the 2014/15 cold season (November–March) produced near-normal precipitation statewide (Fig. 5.1b). In what has since been nicknamed the "snowpack drought" of 2015 (www.ecy.wa.gov/drought/), the drought was more a result of unprecedented warmth (Fig. 5.1c) that caused cold-season precipitation to fall as rain rather than snow on the mountains. A small change in temperature can alter the water balance by reducing the precipitation falling as snow, which results in declined snow water equivalent and summer streamflow (Mote 2006; Stewart et al. 2004). This 2014/15 situation thereby sets an example for the known effect of atmospheric warming on reducing mountain snowpack in the Pacific Northwest (PNW), a known risk that has been reported by a sizable body of research (e.g., Stoelinga et al. 2010; Mote et al. 2014; Abatzoglou et al. 2014).

Reduction in the PNW snowpack also increases the risk of wildfires, the latter of which is evidenced by the remarkable 2015 wildfire season, the largest in the state's history. A Washington Department of Agriculture report (http://agr.wa.gov/FP/Pubs/docs/104-495InterimDroughtReport2015.pdf) estimates the 2015 drought alone has caused more than $335 million (U.S. dollars) of loss for the state's agricultural industry. In this study, we investigate the role natural climate variability played in the 2015 Washington state drought and situate it in the context of anthropogenic climate change.

Data and Model Sources. The observed mean surface air temperatures and precipitation were obtained from monthly records of PRISM's high-resolution spatial climate data (https://climatedataguide.ucar.edu). For the analysis of northern Pacific climate variability, NOAA's extended reconstructed sea surface temperature (SST) v4 was used (Huang et al. 2015). Circulation patterns were based on streamfunction (Ψ) derived from the NCEP–NCAR global wind reanalysis (Kalnay et al. 1996). NCEP's daily two-meter (T_{2m}) air temperature dataset (Kristler et al. 2001) and CPC's unified gauge-based analysis of daily precipitation were used for the estimation of snow-precipitation ratio (S/P) and snow frequency (SF); the latter was also used to characterize dry spells following Gillies et al. (2012). Precipitation was fully classified as snow at $T_{2m} \leq 0°C$. Because the majority of Washington's snowpack is stored in the Cascades, we focused on the cold season of November–March over the mountain ranges outlined in Fig. 5.1a (i.e., all time series were area-averaged from the domain referred to as the Cascades).

Historical and future simulations with the Community Earth System Model version 1 (CESM1) (Hurrell et al. 2013) were analyzed to examine external climate forcing to drought variability in the region and to project possible long-term changes. Thirty ensemble members produced by CESM1 with a spatial resolution of 0.9° longitude × 1.25° latitude through the Large Ensemble Project (Kay et al. 2015) were used. The simulations cover two periods: 1) 1920–2005 with historical forcing, including greenhouse gases, aerosols, ozone, land-use

AFFILIATIONS: Fosu—Department of Plants, Soils, and Climate, Utah State University, Logan, Utah; Wang—Utah Climate Center and Department of Plants, Soils, and Climate, Utah State University, Logan, Utah; Yoon—School of Earth Sciences and Environmental Engineering, Gwangju Institute of Science and Technology, Gwangju, South Korea

DOI:10.1175/BAMS-D-16-0154.1

A supplement to this article is available online (10.1175/BAMS-D-16-0154.2)

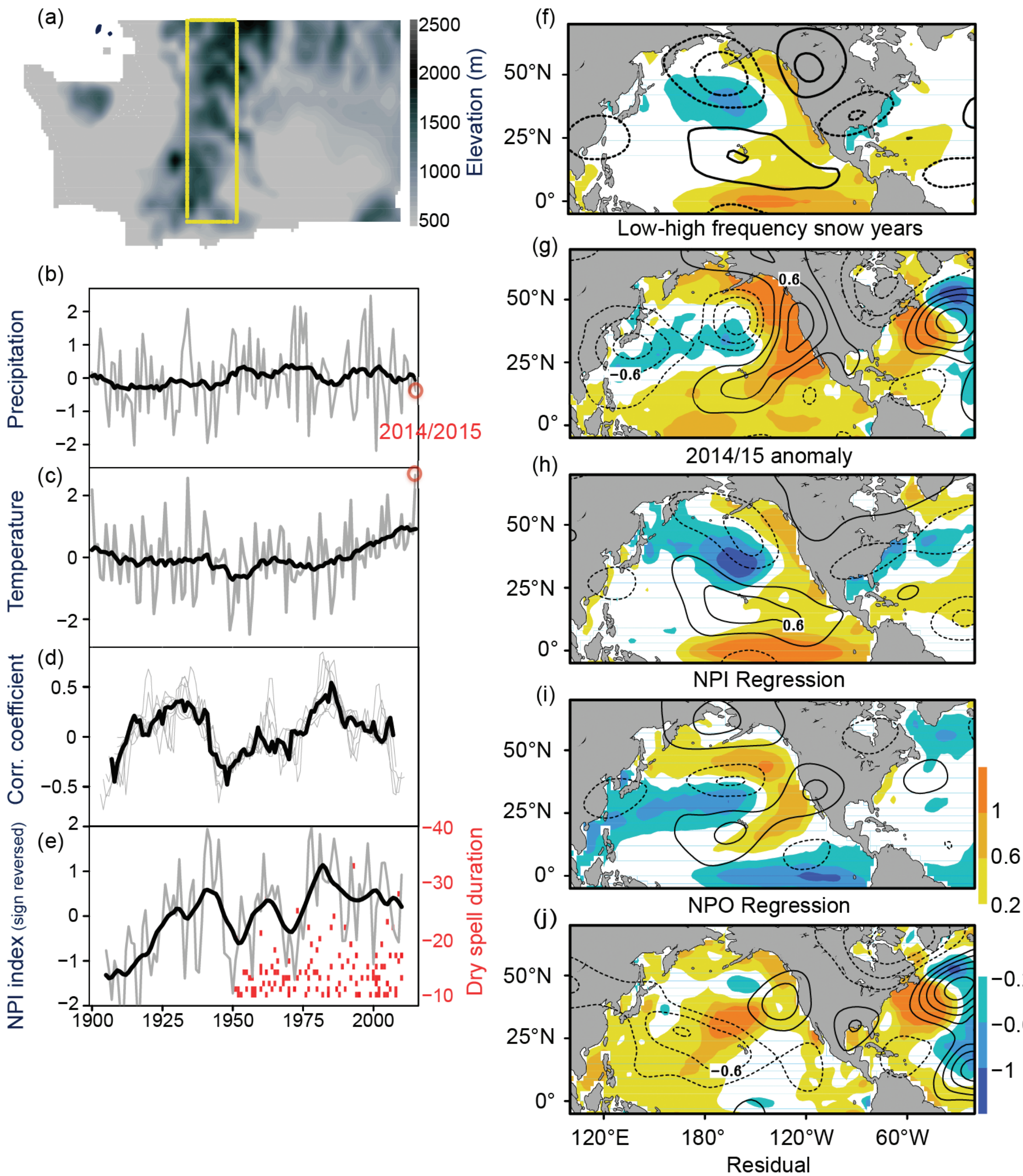

Fig. 5.1. (a) Topographical map of Washington; the yellow box delineates the study domain. (b),(c) Domain averaged time series of normalized cold season precipitation and temperature, both in gray, and their respective 15-year low-pass curves in black. (d) 15-year sliding correlation between P and T, in black. The gray lines show the sliding correlation curves for different windows ranging from 7 to 21 years in 2-year increments. Years on the *x* axis represent the central year of the sliding window. (e) 15-year running mean (black) of the NP index (gray), constructed from the area-weighted sea level pressure over the region 30°–65°N, 160°E–140°W. The NPI sign has been flipped so that positive refers to a deepening of the Aleutian low, which also will correspond to positive PDO phase. The red dots are intense dry spells and their duration (days). (f) Composite differences in cold season circulation (250 mb Ψ in contours, interval: 0.3 10^6 m^2 s^{-1}) and SST (shading) between 31 low and 31 high snow frequency years selected between 1950 and 2014. (g) The observed SST and 250 mb streamfunction anomalies for 2014/15 cold season. (h) A linearly regressed reconstruction of SST and 250 mb streamfunction anomalies related to the NPI, from the 1949/50 cold season to 2013/14, weighed against the strength of the NPI in the 2014/15 season NPI. (i) Same as (h) but for the NPO. (j) Difference between (g) and (h),(i) (i.e., the leftover not linearly explained by the NPI).

change, solar, and volcanic activity, and 2) 2006–80 with RCP8.5 forcing that represents a high-emission pathway (Taylor et al. 2012). The ensemble spread of initial conditions is generated by the commonly used "round-off differences" method (Kay et al. 2014).

Result and Discussion. To examine the unique combination of high temperatures (T) and near-normal precipitation (P) experienced in 2014/15, we computed the correlation between observed P and T over the Cascades. The simultaneous correlation between P and T in the past century has been weak ($r < 0.1$); however, the coherency between P and T appears to fluctuate over time. Figure 5.1d shows the sliding correlation (SCORR) between P and T within various windows ranging from 7 to 21 years, revealing a cyclical pattern in the coherency of P with T on interdecadal timescales. The correlation between P and T was mostly positive during the first third of the century, after which negative correlations prevailed until the late 1970s, then the correlation pattern reversed back to positive. Even though the correlation coefficients are only marginally significant at the peaks and troughs (for the 15-year window the significant SCORR at the 95% interval is .48), the SCORR pattern bears a visual similarity to the low frequency variations within the North Pacific, expressed in Fig. 5.1e by the North Pacific index (NPI; Fig. 5.1e). Calculated from the area-weighted sea level pressure over the region 30°–65°N, 160°E–140°W, the NPI measures the intensity changes of the Aleutian low, which affects cyclone frequency and passages over the PNW (Trenberth and Hurrell 1994). The SCORR pattern mimics the timing of major shifts in the sign of the NPI; a negative regime from 1947–76, with positives dominating from 1925–46 and from 1977 through the present. Since the NPI and the Pacific decadal oscillation (PDO) are significantly correlated, the PDO has a similar interdecadal coherence with P and T (not shown). Here, we focus on the NPI because the PDO is deemed an oceanic response to integrated atmospheric forcing (Newman et al. 2016) and, strictly speaking, should not be directly regarded as a climate driver of the PNW. In Supplemental Table S5.1, we list an array of climate indices and their correlation coefficient with the P–T SCORR using the 15-year window, and both the NPI and PDO stand out as being significant at $p < 0.01$.

Next, the weather processes that encompass the NPI regimes and dry spells in the Cascades are examined. An extreme dry spell was defined as a prolonged period of at least 10 days without substantial precipitation accumulation (< 5 mm). As shown in Fig. 5.1e, more and prolonged dry spells (red dots) tend to occur in the positive NPI regime during which temperature and precipitation tend to be positively correlated. In the opposing phase, less intense dry spells are observed, with negative correlations between temperature and precipitation. A third scenario exists, whereupon a correlation of near zero exists between P and T. The 2014/15 event falls under such zero correlation regime and is evidence that natural climate variability can drive years of extreme warmth and drought even when precipitation is normal.

To understand the circulation and SST patterns associated with wet and dry spells along the Cascades, Fig. 5.1f shows the 250 mb streamfunction and SST differences between low and high snow frequency years. Low snow years are associated with a SST pattern that is analogous to the positive phase of the PDO (or to the interdecadal Pacific oscillation, which has a stronger tropical signal), with a warm tongue of water situated off the coast of California accompanied by an anomalous ridge over the PNW. The 2014/15 circulation anomalies (Fig. 5.1g) produced a similar yet amplified pattern, including the high pressure over the West Coast and a low pressure over northeastern North America. This pair of circulations echo the dipole pattern associated with the 2013/14 California drought (Wang et al. 2014, 2015; Funk et al. 2015) that occurred again in 2015. The circulation anomalies associated with the NPI (Fig. 5.1h) resembles the low snow frequency situation, as was previous documented (e.g., Mote 2006). By comparison, the 2014/15 circulation also bears resemblance to the pattern of North Pacific oscillation (NPO; Rogers 1981) (Fig. 5.1i), with a similar (yet shifted) high pressure ridge over the western United States and warm SST anomalies in the northeastern Pacific. However, the 2014/15 SST anomalies feature an area of much warmer water around the PNW coast, referred to as a "blob" of warmer water consolidated into the PDO's region of ocean fluctuation that was strengthened by the stagnation of high pressure in the Gulf of Alaska (Bond et al. 2015).

To analyze further the collective effects of NPI and NPO on the 2014/15 circulation anomalies, we computed the regression coefficients of streamfunction and SST anomalies with the NPI and NPO from 1949/50 to 2013/14 and weighted the coefficients against the observed values of the 2014/15 season; this led to a statistical estimate of the anomalies that are individually attributable to each mode. Then, a linear "attribution" analysis was carried out by removing the combined regressed patterns of the NPI and NPO from the 2014/15 anomalies (the NPO signal was "regressed out" from the NPI). The residual (Fig. 5.1j) shows a weak swath of warmer SST across the North Pacific with some patches of cool waters, suggesting that the key SST feature in the 2014/15 situation near the PNW has been considerably reduced. The drought-inducing ridge engulfing the West Coast (Fig. 5.1g) was also reduced by more than one half with a displaced center. The residual SST could be explained by possible warming effects of anthropogenic greenhouse gases, as was argued by Weller et al. (2015). Because the Cascades' surface air temperature is significantly correlated with the offshore SST (Supplemental Fig. S5.1), these results hint a collective effect from anthropogenic warming and combined NPI–NPO modulation on the 2014/15 anomaly that led to low snowfall.

The limited length of observational data poses a challenge in verifying the inferred NPI modulation on the fluctuating P–T relationship. We note that the CESM1's 30-member ensemble appears to capture the NPI in both the historical and future runs (using the same definition as in the observation), without any noticeable trend in the RCP8.5 runs (Fig. 5.2a). Likewise, the model does not suggest any perceptible future deviation from the SCORR pattern between P and T (Fig. 5.2b) either. This result suggests that the P–T SCORR and the NPI modulation are natural variability that are not projected to change. Additionally, the spectral coherence between the observed NPI (15-year low-pass) and the 15-year SCORR between P and T was computed. To address uncertainty in the coherence at low frequencies/long periods, we computed the spectral coherence for two periods: 101 (Fig. 5.2c) and 59 (Fig. 5.2d) years. The spectral coherency reveals dominant periodicities at 30–50 years, which is consistent with the NPI's periodicity. The low frequency band should be interpreted with caution owing to the limited data length. Nonetheless, both the historical (Fig. 5.2e) and future (Fig. 5.2f) simulations of the CESM1 reproduced this 30–50-year spectral peak of the coherency. This performance is in line with the CESM1's noted ability in reproducing the broad North Pacific SST variability (Yoon et al. 2015) and the supposed stationarity of the NPI (Fig. 5.2a). Under the future scenario, the model projects an amplified spectral coherency of SCORR with NPI while the frequency remains unchanged. However, the increase in spectral coherency only marginally passes the red noise spectrum (not shown) and therefore does not suggest confidently that global warming would change the correspondence between the P–T regime and the NPI.

In spite of these results, anthropogenic warming continues to pose a threat to the Cascades snowpack as shown in Supplemental Fig. S5.2a. The post-1970 increase in observed T coincides with the rising trend of simulated T, and these correspond to the expected decreasing trend in the projected S/P (Supplemental Fig. S5.2b). However, the accelerated increase in observed temperature and the record warmth in 2014/15 could be an early indication that, even though precipitation in the PNW does not change in the future, the persistent warming will increase the likelihood of a normal P and high T situation like 2014/15 or worse, a high T and low P scenario as suggested in the negative SCORR regime of Fig. 5.1d. In terms of risk assessment, these results suggest that any superimposition of a high T with low P would exacerbate drought, making it potentially more severe than the 2014/15 situation with normal P. The CESM1 projections lend support to such a possibility in the future.

Summary. In the winter of 2014/15, the average temperature along the Cascades was the highest on record and occurred in tandem with the emergence of extremely positive SST anomalies that developed off the coast of the PNW. The high pressure ridge increased the PNW temperatures to a record level while reducing the snow frequency. Diagnostic analysis suggests that a significant portion of the circulation patterns associated with the 2014/15 snowpack drought can be explained by the North Pacific climate variability in the form of the NPI with a modulation from the NPO. Even though the effect of North Pacific climate variability on the PNW is well known (Stoelinga et al. 2010, Mote et al. 2014, Abatzoglou et al. 2014), this study uncovered a unique cyclical relationship between temperature and precipitation that is apparently driven by the low frequency variability of the NPI. This process is especially concerning in light of recent findings that despite little long-term trend in average West Coast precipitation, precipitation may be falling in more concentrated bursts (Prein et al. 2016) due to changes in certain circulation patterns (Swain et al. 2016; Lehmann and Coumou 2015). Under the warming climate, increasing air temperature embedded in stagnated ridge systems off the West Coast (Diffenbaugh et al. 2015) can reduce snowpack

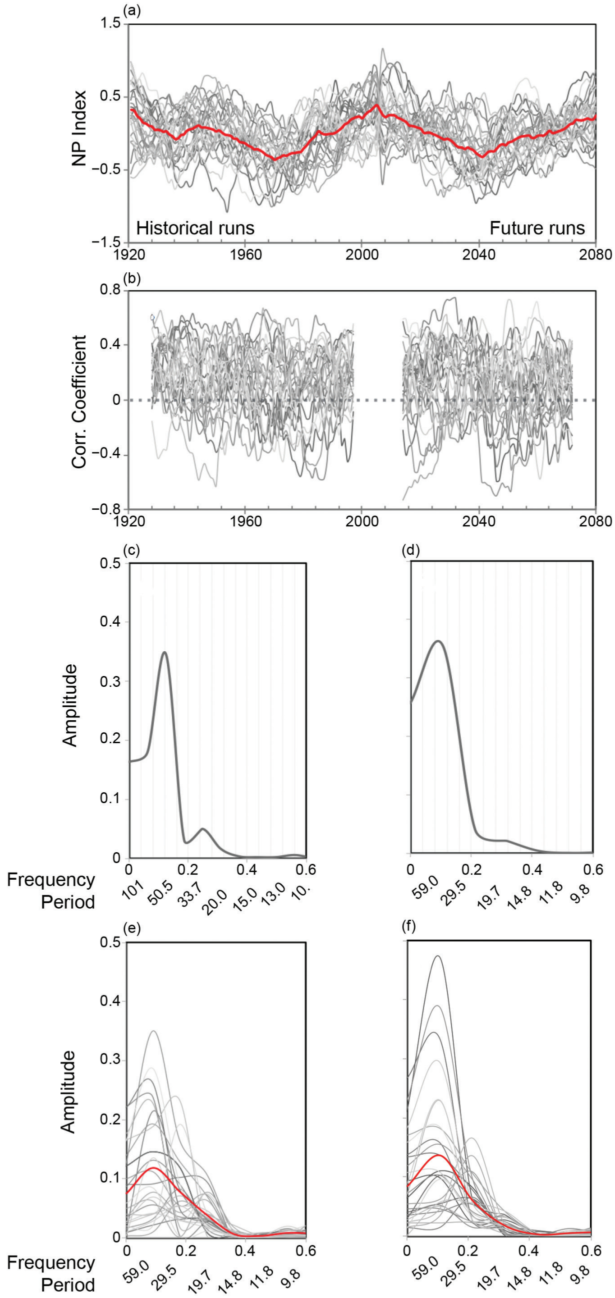

Fig. 5.2. (a) The 15-year running mean of the NPI, constructed as the area-weighted sea level pressure over the region 30°–65°N, 160°E–140°W for 30 CESM1 ensemble members (in gray), and their ensemble mean (in red), for both historical and future RCP8.5 runs, adjoined. (b) 15-year sliding correlation between temperature and precipitation. Years on the *x* axis represent the central year of the 15-year sliding window. (c) Spectral coherence amplitude between the NPI and the 15-year sliding correlation of observed cold season precipitation and temperature from 1908–2008. (d) Same as (c) but from 1928–86. (e),(f) Same as (d) but for CESM1 derived historical (1928–97) and future (2014–72) PDO and SCORR outputs. The minimum number of time steps that could be used was 59 years because of the limited extent of CESM1's future run. As a result, only a comparable number of years in observations could be used to allow for easy comparisons. Similarly, red curves represent the ensemble mean.

even without an apparent precipitation deficit—a situation that was realized in the 2014/15 snowpack drought of Washington.

ACKNOWLEDGEMENTS. This study was supported by WaterSMART Grant R13AC80039, the Utah Agricultural Experiment Station, and partially DE-SC0016605. Yoon was supported by the Global University Project Startup fund project through a grant provided by GIST in 2016. The CESM Large Ensemble Community Project and supercomputing resources are provided by NSF/CISL/Yellowstone.

REFERENCES

Abatzoglou, J. T., D. E. Rupp, and P. W. Mote, 2014: Seasonal climate variability and change in the Pacific Northwest of the United States. *J. Climate,* **27**, 2125–2142, doi:10.1175/JCLI-D-13-00218.1.

Anderson, B., and Coauthors, 2006: 2005 Drought Response Report to the Legislature. Washington Department of Ecology and Water Resources Program, Publication 06-11-001, 56 pp. [Available online at https://fortress.wa.gov/ecy/publications/documents/0611001.pdf.]

Bond, N. A., M. F. Cronin, H. Freeland, and N. Mantua, 2015: Causes and impacts of the 2014 warm anomaly in the NE Pacific. *Geophys. Res. Lett.*, **42**, 3414–3420, doi:10.1002/2015GL063306.

Diffenbaugh, N. S., D. L. Swain, and D. Touma, 2015: Anthropogenic warming has increased drought risk in California. *Proc. Natl. Acad. Sci. USA*, **112**, 3931–3936, doi:10.1073/pnas.142238511.

Funk, C., S. Shukla, A. Hoell, and B. Livneh, 2015: Assessing the contributions of East African and west Pacific warming to the 2014 boreal spring East African drought [in "Explaining Extreme Events of 2014 From a Climate Perspective"]. *Bull. Amer. Meteor. Soc.*, **96 (12)**, S77–S81, doi:10.1175/BAMS-D-15-00106.1.

Gillies, R. R., S.-Y. Wang, and M. R. Booth, 2012: Observational and synoptic analyses of the winter precipitation regime change over Utah. *J. Climate*, **25**, 4679–4698, doi:10.1175/JCLI-D-11-00084.1.

Huang, B., and Coauthors, 2015: Extended reconstructed sea surface temperature version 4 (ERSST.v4). Part I: Upgrades and intercomparisons. *J. Climate*, **28**, 911–930, doi:10.1175/JCLI-D-14-00006.1.

Hurrell, J. W., and Coauthors, 2013: The Community Earth System Model: A framework for collaborative research. *Bull. Amer. Meteor. Soc.*, **94**, 1339–1360, doi:10.1175/BAMS-D-12-00121.1.

Kalnay, E., and Coauthors, 1996: The NMC/NCAR 40-Year Reanalysis Project. *Bull. Amer. Meteor. Soc.*, **77**, 437–471.

Kay, J. E., and Coauthors, 2015: The Community Earth System Model (CESM) large ensemble project: A community resource for studying climate change in the presence of internal climate variability. *Bull. Amer. Meteor. Soc.*, **96**, 1333–1349, doi:10.1175/BAMS-D-13-00255.1.

Kistler, R., and Coauthors, 2001: The NCEP-NCAR 50-year reanalysis: Monthly means CD-ROM and documentation. *Bull. Amer. Meteor. Soc.*, **82**, 247–267.

Lehmann, J., and D. Coumou, 2015: The influence of mid-latitude storm tracks on hot, cold, dry and wet extremes. *Sci. Rep.*, **5**, 17491, doi:10.1038/srep17491.

Mote, P. W., 2006: Climate-driven variability and trends in mountain snowpack in western North America. *J. Climate*, **19**, 6209–6220, doi:10.1175/JCLI3971.1.

Mote, P., A. K. Snover, S. Capalbo, S. D. Eigenbrode, P. Glick, J. Littell, R. Raymondi, and S. Reeder, 2014: Northwest. *Climate Change Impacts in the United States: The Third National Climate Assessment*, J. M. Melillo et al., Eds., U.S. Global Change Research Program, 487–513, doi:10.7930/J04Q7RWX.

Newman, M. and Coauthors, 2016: The Pacific decadal oscillation, revisited. *J. Climate*, **29**, 4399–4427, doi:10.1175/JCLI-D-15-0508.1.

Prein, A. F., G. J. Holland, R. M. Rasmussen, M. P. Clark, and M. R. Tye, 2016: Running dry: The U.S. Southwest's drift into a drier climate state. *Geophys. Res. Lett.*, **43**, 1272–1279, doi:10.1002/2015GL066727.

Rogers, J. C., 1981: The North Pacific oscillation. *J. Climatol.*, **1**, 39–57.

Stewart, I. T., D. R. Cayan, and M. D. Dettinger, 2004: Changes in snowmelt runoff timing in western North America under a `business as usual' climate change scenario. *Climatic Change*, **62**, 217–232, doi:10.1023/B:CLIM.0000013702.22656.e8.

Stoelinga, M. T., M. D. Albright, and C. F. Mass, 2010: A new look at snowpack trends in the Cascade Mountains. *J. Climate*, **23**, 2473–2491, doi:10.1175/2009JCLI2911.1.

Swain, D. L., D. E. Horton, D. Singh, and N. S. Diffenbaugh, 2016: Trends in atmospheric patterns conducive to seasonal precipitation and temperature extremes in California. *Sci. Adv.*, **2**, e1501344, doi:10.1126/sciadv.1501344.

Taylor, K. E., R. J. Stouffer, and G. A. Meehl, 2012: An overview of CMIP5 and the experiment design. *Bull. Amer. Meteor. Soc.*, **93**, 485–498, doi:10.1175/BAMS-D-11-00094.1.

Trenberth, K. E., and J. W. Hurrell, 1994: Decadal atmosphere-ocean variations in the Pacific. *Climate Dyn.*, **9**, 303–319, doi:10.1007/BF00204745.

Wang, S. Y., L. Hipps, R. R. Gillies, and J. H. Yoon, 2014: Probable causes of the abnormal ridge accompanying the 2013–2014 California drought: ENSO precursor and anthropogenic warming footprint. *Geophys. Res. Lett.*, **41**, 3220–3226, doi:10.1002/2014GL059748.

Wang, S. Y. S., W. R. Huang, and J. H. Yoon, 2015: The North American winter "dipole" and extremes activity: A CMIP5 assessment. *Atmos. Sci. Lett.*, **345**, 338–345, doi:10.1002/asl2.565.

Weller, E., S.-K Min, D. Lee, W. Cai, S.-W. Yeh, and J.-S. Kug, 2015: Human contribution to the 2014 record high sea surface temperatures over the western tropical and northeast Pacific Ocean [in "Explaining Extremes of 2014 from a Climate Perspective"]. *Bull. Amer. Meteor. Soc.*, **96 (12)**, S100–S104, doi:10.1175/BAMS-D-15-00055.1

Yoon, J.-H., S.-Y. Wang, R. R. Gillies, B. Kravitz, L. Hipps, and P. Rasch, 2015: Increasing water cycle extremes in California and in relation to ENSO cycle under global warming. *Nature Comm.*, **6**, 8657, doi:10.1038/ncomms9657.